An Experimental Study of Nonlinear Viscoelastic Bushing Model for Axial Mode

Seong Beom Lee*
School of Mechanical and Automotive Engineering, Inje University, 607 Obang-dong, Kimhae, Kyung-nam 621-749, Korea
Jung-Woog Shin
Department of Biomedical Engineering, Inje University, Kimhae, Korea
Alan S. Wineman
Department of Mechanical Engineering, University of Michigan, Ann Arbor, U.S.A.

A bushing is a device used in automotive suspension systems to cushion the force transmitted from the wheel to the frame of the vehicle. A bushing is essentially a hollow cylinder which is bonded to a solid metal shaft at its inner surface and a metal sleeve at its outer surface. The shaft is connected to the suspension and the sleeve is connected to the frame. The cylinder provides the cushion when it deforms due to relative motion between the shaft and sleeve. The relation between the force applied to the shaft or sleeve and its deformation is nonlinear and exhibits features of viscoelasticity. An explicit force-displacement relation has been introduced for multi-body dynamics simulations. The relation is expressed in terms of a force relaxation function and a method of determination by experiments on bushings has been developed. Solutions allow for comparison between the force-displacement behavior by experiments and that predicted by the proposed method. It is shown that the predictions by the proposed force-displacement relation are in very good agreement with the experimental results.

Key Words: Nonlinear Viscoelasticity, Bushing, Force Relaxation Function

1. Introduction

Bushings are structural elements which are used in suspension systems of automobiles and other vehicles. A bushing is, in effect, a hollow cylinder contained between an outer steel cylindrical sleeve and an inner steel cylindrical rod. The steel sleeve and rod are connected to the components an the automotive suspension system and are used to transfer forces from the wheel to the chassis. Bushings are used to reduce shocks and vibrations in this connection. Because those are connected to different parts of the suspension system, the sleeve and rod undergo relative displacements and rotations about axes both parallel and perpendicular to their common centerline. It is the relative displacement that allows for the transmission of force through a bushing.

In analyzing suspension systems that contain bushings, engineers use multi-body dynamics computer codes. In the multi-body dynamics codes, the bushings are typically modeled by using a system of force-displacement relations. Thus, determining a correct force-displacement relation becomes an important task in analyzing a bushing. However, a bushing material is viscoelastic and nonlinear, hence, it causes the relation be-

* Corresponding Author,
E-mail : mechlsb@inje.ac.kr
TEL : +82-55-320-3667; **FAX** : +82-55-324-1723
School of Mechanical and Automotive Engineering, Inje University, 607 Obang-dong, Kimhae, Kyung-nam 621-749, Korea. (Manuscript **Re-ceived** February 12, 2003; **Revised** June 9, 2003)

tween the nonlinear and time dependent corresponding forces and displacements as well as causing coupling between the different modes of response. This viscoelasticity cannot be neglected because it is a mechanism of energy dissipation that is essential for accurate force calculations.

Very few studies of the development of force-displacement relations for bushings have been found in the open literature. Adkins and Gent (1954) developed force-displacement relations for radial, axial, torsional, and conical modes of deformation of bonded cylindrical bushings. Since their results are obtained using the linear elastic theory, the relations do not account for nonlinear, time-dependent effects, or coupling between modes.

Morman et al.(1981) modeled a bushing material as a nonlinear viscoelastic solid. They assumed an appropriate constitutive equation and presented a finite element method for analyzing the response for small amplitude oscillations superposed on large equilibrium deformations. Although their method is important for studying many aspects of bushing response, it does not account for transient response. Thus, it is of limited use in a multi-body dynamics code and both of these works suffer from the disadvantages associated with defining a boundary value problem.

Kim and Youn (2001) proposed a viscoelastic constitutive equation for rubber under small oscillatory load superimposed on large static deformation. The model was extended to a generalized viscoelastic constitutive equation including widely-used Morman's model. Static deformation correction factor was introduced to consider the influence of pre-strain on the relaxation function.

Wineman et al.(1998) suggested a force-displacement relation for single mode bushing response that combines nonlinear dependence on displacement with the time dependence of viscoelasticity. In particular, force is given by a nonlinear single integral expression in terms of a force relaxation function, a bushing property, which represents the force when the bushing is subjected to a step displacement history. They described a process for determining the force relaxation function for a bushing by mechanical testing and data processing and demonstrated this process for radial deformations of bushing.

Lee and Wineman (1999) carried out a study using numerical simulations in order to evaluate how well the force-displacement relation in (Wineman et al., 1998) represented the response of a bushing. They used a constitutive equation developed by McGuirt and Lianis (1970) from experiments on SBR together with the governing field equation of nonlinear viscoelasticity and carried out numerical simulation of the mechanical testing program discussed in (Wineman et al., 1998) using this numerically generated data. They determined an expression for the force relaxation function. Then, they compared preditions of the force-displacement model proposed in (Wineman et al., 1998) with exact predictions of the McGuirt and Lianis model. The comparison was very satisfactory. Thus, the study in (Lee and Wineman, 1999) provided support for the use of force-displacement relation suggested in (Wineman et al., 1998).

The purpose of the present work is to present the results of an experimental program for determining the force relaxation property for a bushing in axial mode. The nonlinear viscoelastic force-displacement relation and method of determining the force relaxation property are outlined in section 2, in order to make this paper as self contained as possible. Experimental results are presented in section 3. The relaxation property is determined in section 4 and its predictive quality is presented in section 5. Section 6 contains final comments.

2. Nonlinear Viscoelastic Force-Displacement Relation

We consider a force-displacement relation for the bushing which combines nonlinear dependence on displacement and time effects of viscoelasticity. The simplest relation which meets these conditions appears to be that introduced by Pipkin and Rogers (1968) for the nonlinear viscoelastic response of polymers. In the current context, it has the form

$$F(t)=R(\Delta(t),0)+\int_0^t \frac{\partial R(\Delta(s),t-s)}{\partial(t-s)}\,ds \quad (1)$$

$F(t)$ is the function of time and represents the force at current time t and s denotes time and has the unit of sec. $R(\Delta, t)$ is a property of the bushing and represents the force at time t due to a step axial displacement of amount Δ applied at time zero. That is, $R(\Delta, t)$ can be interpreted as the axial displacement-dependent force relaxation function. It is reasonable to assume that $R(0^-, t)=0$ and that $R(\Delta, t)$ is a monotonically decreasing function of time t. A typical force relaxation function is shown in Fig. 1.

By applying integration by parts to Eq. (1), the Pipkin-Rogers model can be rewritten as follows:

$$F(t)=R(\Delta(0),t)+\int_0^t \frac{\partial R(\Delta(s),t-s)}{\partial\Delta(s)}\frac{d\Delta(s)}{ds}\,ds \quad (2)$$

Ideally, $R(\Delta, t)$ can be determined by subjecting the bushing to a deformation in which the outer sleeve undergoes a step axial displacement with respect to the inner rod. This ideal process cannot be realized due to the inertia of the testing apparatus. A method which can be used to determine $R(\Delta, t)$ is outlined here.

Consider a displacement which increases at a constant rate to displacement Δ_i in time interval T_j^*, and is then held fixed. It is described by

$$\begin{aligned}\Delta(t)&=\frac{\Delta_i}{T_j^*}t, \qquad 0\le t\le T_j^*,\\ &=\Delta_i, \qquad T_j^*\le t\end{aligned} \quad (3)$$

where T_j^* is defined as the rise time, which is the time where the displacement rate in displacement vs. time function changes from constant to zero.

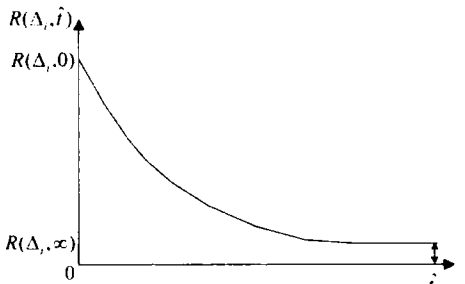

Fig. 1 Displacement-dependent force relaxation function for $\Delta(t)=\Delta_i$

Let this ramp to constant displacement history be denoted by $\Delta(\Delta_i, T_j^*, t)$. The force output history corresponding to this ramp to constant displacement history can be expected to increase monotonically until time T_j^*, and then relax for times $t>T_j^*$, when the displacement is held constant. As T_j^* approaches zero, the ramp to constant displacement control test approaches the step displacement control test. Moreover, as T_j^* approaches zero, the force response can be expected to approach the displacement-dependent force relaxation function $R(\Delta_i, t)$. In order to show this, let Eq. (3) be substituted into Eq. (2), and consider any time $t\ge T_j^*$. Since $R(\Delta(0), t)=R(0, t)=0$ and $d\Delta(s)/ds=0$, $s\ge T_j^*$,

$$F(t)=\int_0^{T_j^*}\frac{\partial R(\Delta(s),t-s)}{\partial\Delta(s)}\frac{d\Delta(s)}{ds}\,ds \quad (4)$$

This force will be denoted by $\tilde{R}(\Delta_i, t, T_j^*)$.

In Eq. (4), let the integration variable be changed from s to Δ, $\Delta=\Delta_i s/T_j^*$. Also, let $t=T_j^*+\hat{t}$, where $\hat{t}$ denotes a fixed time measured from T_j^*, when the displacement is held constant. Then, Eq. (4) becomes

$$\tilde{R}(\Delta_i,\hat{t},T_j^*)=\int_0^{\Delta_i}\frac{\partial R\left(\Delta,\hat{t}+T_j^*\left(1-\frac{\Delta}{\Delta_i}\right)\right)}{\partial\Delta}\,d\Delta \quad (5)$$

As T_j^* approaches zero, Eq. (5) becomes

$$\lim_{T_j^*\to 0}\tilde{R}(\Delta_i,\hat{t},T_j^*)=\int_0^{\Delta_i}\frac{\partial R(\Delta,\hat{t})}{\partial\Delta}\,d\Delta=R(\Delta_i,\hat{t}) \quad (6)$$

Let Δ_i, $i=1, 2, 3, \cdots, n_\Delta$ be a set of axial displacements and let T_j^*, $j=1, 2, 3, \cdots, n_{T^*}$, be the set of rise times at which the ramp to constant displacement history described in Eq. (3) is carried out.

Consider a fixed value of displacement Δ_i and let the rise time T_j^* decrease as j increases, that is, $T_{j+1}^*<T_j^*$. A set of such histories for T_j^*, $(j=1, 2, 3)$, is shown in Fig. 2.

Because of experimental limitations, the limit $T_j^*\to 0$ can not be reached. This difficulty is approached as follows. Let $\tilde{R}_{\exp}(\Delta_i, T_j^*, t)$ denote the experimentally determined force history

response at time $t \geq T_j^*$. When the slope of ramp to constant displacement history $\Delta(\Delta_i, T_j^*, t)$ changes from positive to zero at the rise time T_j^*, the slope of the force-time response changes from positive to negative at time T_j^*. Let $\hat{t}$ be a fixed time interval measured from this break in the slope at time T_j^*, that is, $t=\hat{t}+T_j^*$. For the rise times T_j^*, $j=1, 2, 3, \cdots, n_T$, $\tilde{R}_{\exp}(\Delta_i, T_j^*, T_j^*+\hat{t})$ denotes a set of data points associated with time $\hat{t}$ and displacement Δ_i.

Figure 3 shows plots of the experimentally determined force output $\tilde{R}_{\exp}(\Delta_i, T_j^*, t)$ versus t, with a fixed value at $\hat{t}$ for several rise times T_j^*. Moreover, it shows a plot of $\tilde{R}_{\exp}(\Delta_i, T^*, T^*+\hat{t})$ versus T^* for three rise times T_j^*. Let $\tilde{R}_{fit}(\Delta_i, \hat{t}, T^*)$ denote a function of T^*, which is fit to this set of data points, so that

$$\tilde{R}_{fit}(\Delta_i, \hat{t}, T_j^*)=\tilde{R}_{\exp}(\Delta_i, T_j^*, T_j^*+\hat{t}), \quad T_j^*, j=1, 2, 3, \cdots, n_T^* \tag{7}$$

$\tilde{R}_{fit}(\Delta_i, \hat{t}, T^*)$ is used to extrapolate the data for T_j^*, $j=1, 2, 3, \cdots, n_T^*$ to $T_j^*=0$. In particular, it is assumed that

$$\lim_{T^*\to 0}\tilde{R}_{fit}(\Delta_i, \hat{t}, T^*)=\tilde{R}_{fit}(\Delta_i, \hat{t}, 0) =\lim_{T_j^*\to 0}\tilde{R}_{\exp}(\Delta_i, T_j^*, T_j^*+\hat{t})=R(\Delta_i, \hat{t}) \tag{8}$$

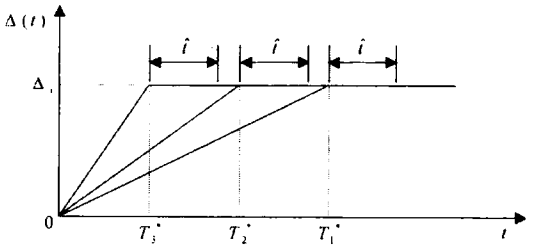

Fig. 2 Ramp to constant displacement history (input)

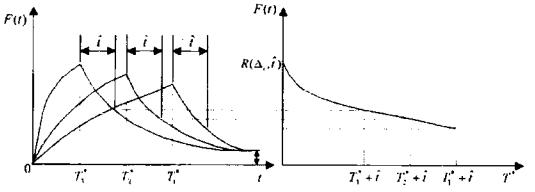

Fig. 3 Force output for ramp to constant displacement control tests

A choice for $\tilde{R}_{fit}(\Delta_i, \hat{t}, T^*)$ was determined by considering the extrapolation. For a given displacement Δ_i and a fixed time interval $\hat{t}$, $\tilde{R}_{fit}(\Delta_i, \hat{t}, T^*)$ is defined by the relation

$$\tilde{R}_{fit}(\Delta_i, \hat{t}, T^*)=C_1+C_2\left(\frac{1-e^{-(T^*/\tau)}}{(T^*/\tau)}\right) \tag{9}$$

C_1, C_2, and τ are constants which are found by minimizing

$$\sum_{j=1}^{n_T^*}\left(\left(C_1+C_2\left(\frac{1-e^{-(T_j^*/\tau)}}{(T_j^*/\tau)}\right)\right)-\tilde{R}_{\exp}(\Delta_i, T_j^*, T_j^*+\hat{t})\right)^2 \tag{10}$$

By substituting Eq. (9) into Eq. (8) and using the result $\lim_{T^*\to 0}[1-e^{-(T^*/\tau)}/(T^*/\tau)]=1$, it is found that

$$R(\Delta_i, \hat{t})=C_1+C_2 \tag{11}$$

The process indicated in Eqs. (10) and (11) can be carried out on any specified set of displacement Δ_i and times $\hat{t}$. This process gives $R(\Delta_i, \hat{t})$, the force at time $\hat{t}$ due to an axial displacement Δ_i. By repeating this process for a range of displacement Δ_i and time $\hat{t}$, the relaxation function can be determined as Fig. 1.

3. Experimental Results

In this paper, only axial mode deformations were considered. Reference and current configurations in axial mode are shown in Fig. 4.

Experiments were carried out on an MTS 858 (2.5ton) testing machine and bushings were provided by a commercial company. The bushing was fixed at its outer radius and the inner rod

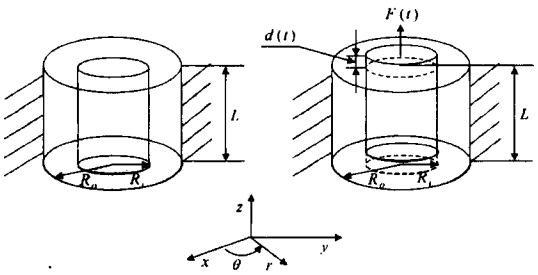

Fig. 4 Reference and current configurations in axial mode

Table 1 Given displacement histories for experiment

d_i \ T_j^*	T_1^*	T_2^*	T_3^*	T_4^*	T_5^*	T_6^*
d_1=4 mm	8 sec.	6 sec.	4 sec.	2 sec.	1 sec.	0.5 sec.
d_2=5 mm	8 sec.	6 sec.	4 sec.	2 sec.	1 sec.	0.5 sec.
d_3=6 mm	8 sec.	6 sec.	4 sec.	2 sec.	1 sec.	0.5 sec.
d_4=7 mm	8 sec.	6 sec.	4 sec.	2 sec.	1 sec.	0.5 sec.
d_5=8 mm	8 sec.	6 sec.	4 sec.	2 sec.	1 sec.	0.5 sec.

was subjected to a displacement $d(t)$ as indicated in Fig. 4. In particular, the ramp to constant displacement histories were as follows:

$$\begin{aligned} d(t) &= \frac{d_i}{T_j^*}\, t, \qquad 0 \le t \le T_j^* \\ &= d_i, \qquad T_j^* \le t \le 120 \text{ sec.} \\ i &= 1, 2, 3, 4, 5, \quad j = 1, 2, 3, 4, 5, 6 \end{aligned} \tag{12}$$

The set of rise times T_j^* and displacements d_i are shown in Table 1.

While factors such as aging, amplitude and frequency of loading, and temperature do affect conditioning and degradation of the material over time, they were not considered in this study. It can be considered in the future study.

The ideal type of bushing test is step displacement control test. However, due to inertia of the testing equipment, a true step displacement control test is not physically possible. Therefore, a ramp to constant displacement was used instead of a step displacement. The test controller was programmed to increase displacement at a constant rate during a period from time zero to a rise time T^* and hold it fixed at d_i after the rise time T^*. As the rise time T^* of the ramp for each test decreases, the ramp to constant displacement control test approaches a step displacement control test. Thirty ramp to constant displacement control tests in Table 1 were performed until t= 120 sec. A typical force output for d_i=8 mm is shown in Fig. 5.

For each of the ramp to constant displacement control tests, the peak force occurs when the prescribed displacement changes from increasing to being held constant and the peak load is the greatest at the shortest rise time. The force relaxes to an equilibrium during the period in which the displacement remains constant. This response is found in typical viscoelastic materials.

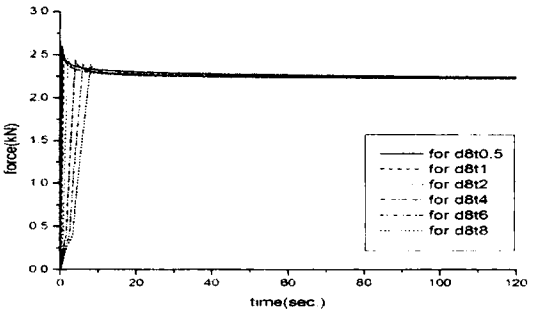

Fig. 5 Force output for d_i=8 mm (from experiment)

4. Mathematical Representation of $R(d, t)$ for the Pipkin-Rogers Model

In this section, we consider a relation in which the force is expressed explicitly in terms of the displacement history, namely, the Pipkin-Rogers model presented in section 2. For present purposes, we use the form of the Pipkin-Rogers model in Eq. (2). Using the force extrapolation method described in section 2 for each of d_i= 4, 5, 6, 7, 8 mm, the constant values of the force relaxation functions for $0 \le t \le 100$ sec. are obtained. The extrapolation process used was carried for $0 \le t \le 60$ sec. because the experiments showed the force was constant for $t \ge 60$ sec. They are shown in Fig. 6.

Note that the plots in Fig. 6 were produced by specifying data points and letting the computer graphics program produce a smooth curve. Because the axial force is odd in the axial displacement, the polynomial contains only odd powers

of displacement d. Thus, $R(d, t)$ was represented as follows:

$$R(d, t)=dG_1(t)+d^3G_3(t) \tag{13}$$

Since $G_1(t)$ and $G_3(t)$ are the functions of time and the coefficients of d and d^3 respectively, Eq. (13) shows that $R(d, t)$ can be expressed explicitly by time and displacement.

Let $d^{(\gamma)}$ be the value of a step displacement, i.e., $d^{(1)}=4$ mm, $d^{(2)}=5$ mm, $d^{(3)}=6$ mm, $d^{(4)}=7$ mm, $d^{(5)}=8$ mm. Then, the displacement-dependent force relaxation functions for $d^{(\gamma)}$ represent a data set which can be used for finding $G_1(t_a)$ and $G_3(t_a)$, $t_a=(a-1)/10$ sec., $a=1, 2, 3, \cdots, 601$. and shown in Fig. 6. Since time interval is defined as $\Delta t=0.1$ sec., the number of data point is 601.

Then,

$$R(d^{(\gamma)}, t_a)=d^{(\gamma)}G_1(t_a)+(d^{(\gamma)})^3G_3(t_a) \tag{14}$$

where $t_a=(a-1)/10$ sec., $a=1, 2, 3, \cdots, 601$., $\gamma=1, 2, 3, 4, 5$.

Then, $G_1(t_a)$ and $G_3(t_a)$ were determined so as to minimize the least-squares error. The least-squares error is defined as follows:

$$E(t_a)=\sum_{\gamma=1}^{5}(R(d^{(\gamma)}, t_a)-d^{(\gamma)}G_1(t_a)-(d^{(\gamma)})^3G_3(t_a))^2 \tag{15}$$

where $t_a=(a-1)/10$ sec., $a=1, 2, 3, \cdots, 601$.

The coefficients, $G_1(t_a)$ and $G_3(t_a)$ are obtained at a set of times t_a for $t_a=(a-1)/10$ sec., $a=1, 2, 3, \cdots, 601$. $G_1(t_a)$ and $G_3(t_a)$ are shown in Fig. 7.

Note that the plots were produced by specifying data points and letting the computer graphics program produce a smooth curve. These data can be represented by sums of exponential functions,

$$\tilde{G}_i(t)=C_{i1}+C_{i2}e^{-t/\tau_{i2}}+C_{i3}e^{-t/\tau_{i3}} \tag{16}$$

where $i=1, 3$. The parameters ($C_{i\alpha}$, $\tau_{i\beta}$, $\alpha=1, 2, 3$, $\beta=2, 3$) were found by using the nonlinear least-squares method and are shown in Table 2.

Let the relative error of the fit of $\tilde{G}_i(t)$ to the data represented by $G_i(t)$ be defined by

$$E_i=\frac{\| \tilde{G}_i(t_a)-G_i(t_a) \|_2}{\| G_i(t_a) \|_2}\times 100(\%)$$
$$=\frac{\sqrt{\sum_{a=1}^{601}(\tilde{G}_i(t_a)-G_i(t_a))^2}}{\sqrt{\sum_{a=1}^{601}(G_i(t_a))^2}}\times 100(\%) \tag{17}$$

where $t_a=(a-1)/10$ sec., $a=1, 2, 3, \cdots, 601$., $i=1, 3$.

The relative errors are $E_1=0.01\%$, $E_3=0.05\%$.

Table 2 Parameters related to displacement-dependent force relaxation function

i	C_{i1}	C_{i2}	C_{i3}	τ_{i2}	τ_{i3}
1	1.6222	0.0586	0.1860	33.9885	2.8163
3	2.0179	0.1994	0.2814	38.3531	1.4039

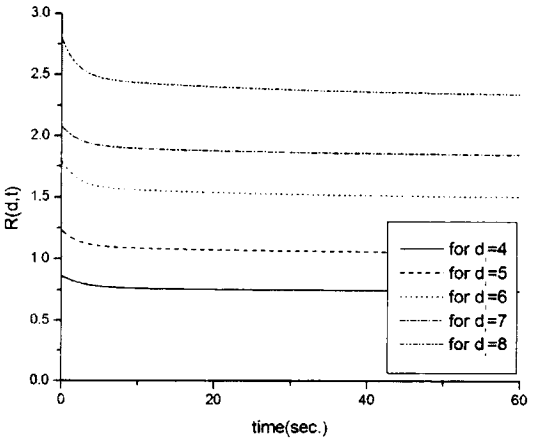

Fig. 6 Displacement-dependent force relaxation function for $d_i=4, 5, 6, 7, 8$ mm

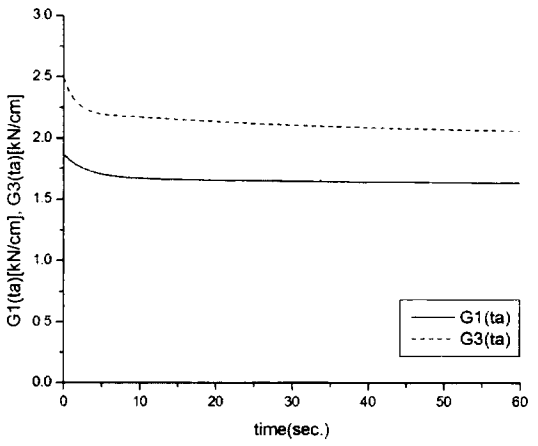

Fig. 7 Coefficients of $R(d, t)$: $t_a=(a-1)/10$ sec., $a=1, 2, 3, \cdots, 601$.

Therefore, the data $(G_i(t_a),\ i=1,\ 3,\ t_a=0,\ 0.1,\ 0.2,\ 0.3,\ \cdots,\ 60$ sec.) can be approximated by $(\tilde{G}_i(t),\ i=1,\ 3)$ in Eq. (16) with a relative error below 0.1%. Plots of the points given by the expression in Eq. (16) and the data set are nearly indistinguishable.

Finally, the complete form of the Pipkin-Rogers model for the axial mode obtained by combining Eqs. (2), (13), and (16) is as follows:

$$F(t)=R(d(0),\ t)+\int_0^t \left\{ \frac{\partial R(d(s),\ t-s)}{\partial d(s)} \frac{d}{ds}(d(s)) \right\} ds \tag{18}$$

where

$$R(d(s),\ t)=[C_{11}+C_{12}e^{-t/\tau_{12}}+C_{13}e^{-t/\tau_{13}}]d(s)+[C_{31}+C_{32}e^{-t/\tau_{32}}+C_{33}e^{-t/\tau_{33}}](d(s))^3 \tag{19}$$

where $C_{i\alpha}$, $\tau_{i\beta}$, $i=1,\ 3$, $\alpha=1,\ 2,\ 3$, $\beta=2,\ 3$ are in Table 2.

5. Predictive Quality of the Pipkin-Rogers Model

The Pipkin-Rogers model in the previous section was introduced as an approximation to the real bushing model. The purpose of this section is to discuss the predictive capability of the Pipkin-Rogers model to the real model. Both the experimental results and the Pipkin-Rogers model were used to determine the force responses to specified displacement histories for $0\le t\le 60$ sec. Since both the Pipkin-Rogers outputs and experimental results are vectors, for evaluation purposes, the relative error E is defined by

$$E=\frac{\|(\textit{the Pipkin and Rogers outputs})-(\textit{Experimental results})\|_2}{\|(\textit{Experimental results})\|_2}\times 100(\%) \tag{20}$$

The particular displacement histories for the experiment and the Pipkin-Rogers model are

$$\begin{aligned} d(t)&=\frac{d_i}{T_j^*}\,t, && 0\le t\le T_j^* \\ &=d_i, && T_j^*\le t\le 60 \text{ sec.} \end{aligned} \tag{21}$$

$$i=1,\ 2,\ 3,\ 4,\ 5,\quad j=1,\ 2,\ 3,\ 4,\ 5,\ 6$$

$$\begin{pmatrix} d_i=4,\ 5,\ 6,\ 7,\ 8 \text{ mm} \\ T_j^*=0.5,\ 1,\ 2,\ 4,\ 6,\ 8 \text{ sec.} \end{pmatrix}$$

The force outputs from the Pipkin-Rogers model for $d_i=8$ mm are shown in Fig. 8.

For comparison, the experimental results for $0\le t\le 60$ sec. at $d_i=8$ mm shown in Fig. 5, are modified until t=60 sec. and are shown again in Fig. 9.

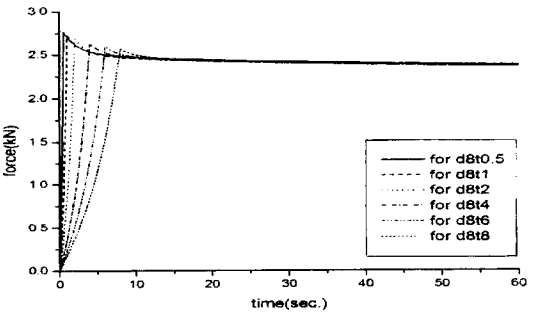

Fig. 8 Force output for $d_i=8$ mm (from Pipkin-Rogers model)

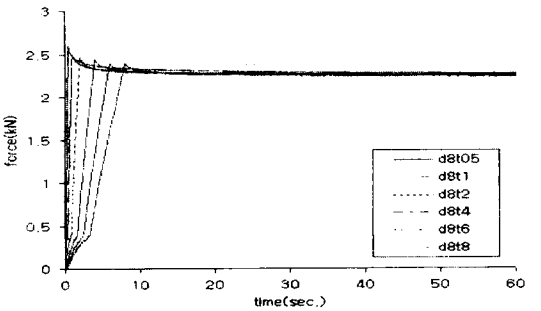

Fig. 9 Force output for $d_i=8$ mm (from experiment)

Table 3 Relative errors of the Pipkin-Rogers model to the experimental results

time (sec.) / displacement (mm)	$T^*=0.5$	$T^*=1$	$T^*=2$	$T^*=4$	$T^*=6$	$T^*=8$
$d_i=4$	9.59%	5.86%	6.9%	7.71%	9.01%	9.07%
$d_i=5$	4.07%	3.15%	3.66%	4.2%	5.02%	5.88%
$d_i=6$	1.54%	1.3%	1.67%	2.47%	3.31%	3.61%
$d_i=7$	4.04%	1.46%	1.5%	1.69%	1.99%	2.3%
$d_i=8$	5.99%	6.24%	6.57%	6.34%	6.89%	6.8%

For all rise times T^* and d_i=4, 5, 6, 7, 8 mm, the comparison between Pipkin-Rogers outputs and experimental results for $0 \leq t \leq 60$ sec. are carried out. And, the relative errors of the Pipkin-Rogers model to the experimental results are defined as Eq. (20) and are shown in Table 3.

For the thirty cases considered, the relative errors are below 10% and the Pipkin-Rogers model appears to provide satisfactory agreement with experimental results.

6. Summary and Conclusions

The force-displacement relation for axial mode response of a bushing has been studied experimentally. The proposed relation is explicit, but approximate, and is expressed in terms of a force relaxation property determined from experimental results. The force relaxation property in the explicit force-displacement relation was determined by a method which extrapolates results obtained from experiment. However, since this results can be used for the same bushing model in axial mode experiment was carried out, it is not possible to use all of bushing.

However, the success of the present study for axial mode response suggests that the same approach is applied to other bushings and other modes, such as torsional or radial modes. The development of an explicit force-displacement relation for coupled mode response should also be considered. These are treated in separate studies.

Acknowledgment

The Author would like to acknowledge the financial support of Central Corporation.

References

Adkins, J. E. and Gent, A. N., 1954, "Load-Deflection Relations of Rubber Bush Mountings," *British Journal of Applied Physics*, Vol. 5, pp. 354~358.

Kim, Bong-Kyu and Youn, Sung-Kie, 2001, "A Viscoelastic Constitutive Model of Rubber Under Small Oscillatory Loads Superimposed on Large Static Deformation," *Transactions of KSME*, Vol. 25, No. 4, pp. 619~628.

Lee, S. and Wineman, A. S., 1999, "A Model for Non-Linear Viscoelastic Axial Response of an Elastomeric Bushing," *International Journal of Non-Linear Mechanics*, Vol. 34, pp. 779~793.

McGuirt, C. W., Lianis, G., 1970, "Constitutive Equations for Viscoelastic Solids Under Finite Uniaxial and Biaxial Deformations," *Transactions of the Society of Rheology*, Vol. 14, No. 2, pp. 117~134.

Morman, K. N., Jr., Kao, B. G. and Nagtegaal, J. C., 1981, "Finite Element Analysis of Viscoelastic Elastomeric Structures Vibrating About Nonlinear Statically Stressed Configurations," *Fourth International Conference on Vehicle Structural Mechanics, Society of Automotive Engineers, Detroit, Michigan*, pp. 83~92.

Pipkin, A. C. and Rogers, T. G., 1968, "A Non-Linear Integral Representation for Viscoelastic Behavior," *Journal of the Mechanics and Physics of Solids*, Vol. 16, pp. 59~72.

Wineman, A. S., VanDyke, T. and Shi, S., 1998, "A Nonlinear Viscoelastic Model for one Dimensional Response of Elastomeric Bushings," *International Journal of Mechanical Sciences*, Vol. 40, pp. 1295~1305.